

Characterisation of products of tricalcium silicate hydration in the presence of heavy metals

Q.Y. Chen^{a,*}, C.D. Hills^b, M. Tyrer^c, I. Slipper^b, H.G. Shen^a, A. Brough^d

^a School of Environmental Science and Engineering, Donghua University, Shanghai 200051, PR China

^b Centre for Contaminated Land Remediation, School of Science, University of Greenwich, Pembroke, Chatham Maritime, Kent ME4 4TB, UK

^c Department of Materials, Imperial College of Science, Technology and Medicine, London SW7 4AZ, UK

^d Department of Civil Engineering, University of Leeds, Leeds LS2 9JT, UK

Received 30 September 2006; received in revised form 21 January 2007; accepted 22 January 2007

Available online 6 February 2007

Abstract

The hydration of tricalcium silicate (C_3S) in the presence of heavy metal is very important to cement-based solidification/stabilisation (s/s) of waste. In this work, tricalcium silicate pastes and aqueous suspensions doped with nitrate salts of Zn^{2+} , Pb^{2+} , Cu^{2+} and Cr^{3+} were examined at different ages by X-ray powder diffraction (XRD), thermal analysis (DTA/TG) and ^{29}Si solid-state magic angle spinning/nuclear magnetic resonance (MAS/NMR). It was found that heavy metal doping accelerated C_3S hydration, even though Zn^{2+} doping exhibited a severe retardation effect at an early period of time of C_3S hydration. Heavy metals retarded the precipitation of portlandite due to the reduction of pH resulted from the hydrolysis of heavy metal ions during C_3S hydration. The contents of portlandite in the control, Cr^{3+} -doped, Cu^{2+} -doped, Pb^{2+} -doped and Zn^{2+} -doped C_3S pastes aged 28 days were 16.7, 5.5, 5.5, 5.5, and $<0.7\%$, respectively. Heavy metals co-precipitated with calcium as double hydroxides such as $(Ca_2Cr(OH)_7 \cdot 3H_2O)$, $(Ca_2(OH)_4Cu(OH)_2 \cdot 2H_2O)$ and $(CaZn_2(OH)_6 \cdot 2H_2O)$. These compounds were identified as crystalline phases in heavy metal doping C_3S suspensions and amorphous phases in heavy metal doping C_3S pastes. ^{29}Si NMR data confirmed that heavy metals promoted the polymerisation of C–S–H gel in 1-year-old of C_3S pastes. The average numbers of Si in C–S–H gel for the Zn^{2+} -doped, Cu^{2+} -doped, Cr^{3+} -doped, control, and Pb^{2+} -doped C_3S pastes were 5.86, 5.11, 3.66, 3.62, and 3.52. And the corresponding Ca/Si ratios were 1.36, 1.41, 1.56, 1.57 and 1.56, respectively. This study also revealed that the presence of heavy metal facilitated the formation of calcium carbonate during C_3S hydration process in the presence of carbon dioxide.

© 2007 Published by Elsevier B.V.

Keywords: C_3S ; Hydration; Heavy metal; C–S–H gel; Polymerisation

1. Introduction

Alite is the most abundant phase of Portland cement and plays an important role in hydration of cementitious materials. As tricalcium silicate (C_3S) is the pure form of alite, C_3S hydration has been extensively investigated and a divergence of opinions exists in literatures [1–3]. As well known, C_3S is thermodynamically unstable due to non-regular co-ordination, and its reactivity with water results in the formation of calcium silicate hydrate (C–S–H) gel and portlandite. The gel model and crystal model have been forwarded to explain hydration of C_3S and cement:

- In the gel model, a membrane of calcium silicate hydrate (C–S–H) gel is formed on the surfaces of C_3S , when C_3S grains contact with water. This membrane permits the inward flow of water molecules and the outward migration of mainly Ca^{2+} and silicate ions due to the difference of osmotic potential on both sides of the membrane. Portlandite forms and accumulates on the fluid side of the membrane.
- In the crystal model, calcium silicate mineral dissociates into charged silicate and calcium ions. The charged silicate ions then concentrate as a thin silicon rich layer on the surface of C_3S grains. The nucleation and growth of hexagonal crystals of calcium hydroxide fill up the spaces and cavities between the grains. Meanwhile, particles of C–S–H precipitate out of water onto the silicate-rich layer on the C_3S grains and gradually form needles or spines.

* Corresponding author. Tel.: +86 21 6779 2540; fax: +86 21 6779 2522.
E-mail address: qychen@dhru.edu.cn (Q.Y. Chen).

The structure and molecular composition of C–S–H gel are problematical at present [1,4]. A number of essential models regarding the structure of C–S–H gel, for example, Taylor's model [4], Glasser's isolated disilicate model [5], and Richardson–Groves' linear single chain model [6–9] have been put forward. Unfortunately, Glasser's model cannot explain Q^2 species in hydrated C_3S pastes. Taylor's model is based on the assumption that C–S–H gel relates to the structures of at least two kinds of crystalline calcium silicate hydrate minerals such as tobermorite or jennite. However, C–S–H gel is a highly disordered amorphous phase in cement or C_3S pastes and there is no convincing evidence that structure of C–S–H gel generated from C_3S or cement hydration stacks like the crystalline structure of calcium silicate hydrates [5]. Additionally, for high disordered amorphous C–S–H gel, it is unlikely that silicon only adopts numbers of $(3m - 1)$ (m is an integer), as indicated in the Richardson–Groves' model. It is likely that a continuous range of chemical composition of C–S–H gel may exist in C_3S or cement pastes [5].

Since 1970s, cement-based solidification/stabilisation (s/s) has been widely used in the treatment of industrial residues, sewage sludge and soil contaminated by heavy metal compounds [10,11]. The s/s technology is now recognised as one of the most effective management techniques of reducing the mobility of toxic heavy metal pollutants. Recently, the amount of modern green cement made from wastes increases dramatically and may contain significant quantities of heavy metals derived from raw materials and fuels. These metals are incorporated in the clinker phases during the burning process of cement [12,13] and affect the hydration behaviour of cement as well as the durability of concrete.

There are mounting interests in understanding interactions of heavy metal ions and cement phases during cement hydration process. The characterisation of hydration products in the presence of heavy metals has received considerable attention [14,15]. A number of models, including the double layer model, the triple layer model and the charge-dispersal model, have been developed to understand the intrinsic mechanism involved in cement-based s/s processes and heavy metal-bearing cementitious materials [2,3].

In the present work, hydrated C_3S pastes and aqueous suspensions doped with heavy metal nitrates have been used in order to characterise hydration products of C_3S in the presence of heavy metal. Nitrate salts were chosen because of their high solubility in aqueous solution and because nitrate anion has little

effect on the hydration of C_3S and cement [16,17]. The effects of these metals on phase development of C_3S hydration were evaluated up to 1 year of age by X-ray powder diffraction (XRD), thermal analyses (DTA/TG) and ^{29}Si solid-state magic angle spinning/nuclear magnetic resonance (MAS/NMR) techniques. The molecular models of C–S–H gel and heavy metal incorporation mechanism in C–S–H have been discussed based on the experimental results.

2. Experimental

2.1. Materials

Tricalcium silicate was synthesised from $CaCO_3$ and SiO_2 (Aldrich Chemical Company, purity >98%). A 3:1 molar ratio mixture of $CaCO_3$ and SiO_2 was ground to a fine powder in a ceramic ball mill, pelletised and then sintered at $1500^\circ C$ for 2 h. These cycles of preparation were repeated until no XRD peaks of free CaO was detected (Fig. 1). The diffractogram of C_3S obtained conforms to that of a typical C_3S described in references [1,18].

Solutions of Cu, Cr, Pb and Zn were prepared from their respective standard reagent grade metal nitrates salts (BCD Ltd.). Each metal salt, $Cu(NO_3)_2 \cdot 3H_2O$, $Zn(NO_3)_2 \cdot 6H_2O$, $Cr(NO_3)_3 \cdot 9H_2O$ and $Pb(NO_3)_2$, was dissolved in de-ionised water at a concentration of 5% (w/w) or 10% (w/w) (by heavy metal ion weight, assuming ideal stoichiometry) for various uses. At a concentration of 5% (w/w), mole concentrations for Cu, Zn, Cr and Pb were 0.79, 0.76, 0.96 and 0.24 M, respectively. For the interest of practical application, heavy metal doping load to C_3S varied by weight to investigate effects of heavy metals on C_3S hydration in this study.

2.2. Methods

2.2.1. C_3S pastes

In the preparation of hydrated pastes of C_3S containing a metal salt, 30 g of C_3S were mixed with a solution of heavy metal nitrate at a concentration of 10% (w/w) (as heavy metal ions) at a solid/liquid ratio of 10:4. The heavy metal content in the C_3S pastes (doping load of heavy metal) was 4% (w/w). For the control sample, C_3S was added to de-ionised water at the same solid/water ratio. These samples were kept in plastic screw top bottles in \varnothing 50 mm (in diameter) at the laboratory ambient temperature of around $17^\circ C$.

2.2.2. C_3S suspensions

In C_3S pastes, amorphous structures of heavy compounds may tend to form, possibly because the nucleation and aggregation occur too fast and species lack sufficient mobility to undergo proper orientation and alignment before bonding into a structure. As amorphous compounds are difficult to identified directly, in this work, the suspensions of C_3S with heavy metals were used to create the more favourable conditions for heavy metal compound crystallising.

The heavy metal nitrate solution with a concentration of 5% (w/w) (as heavy metals) was added to 10 g of C_3S clinker at a

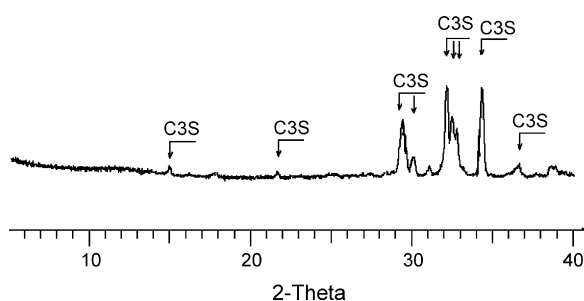


Fig. 1. The XRD pattern of C_3S .

solid/liquid ratio of 1:3. The initial concentration of heavy metal in C_3S suspensions was 50 g/l, but after 30 min of hydration, the heavy metal concentration decreased to <1 mg/l due to the high pH media resulted from C_3S hydration. The doping load of heavy metal to C_3S was 3/20 g/g, i.e. 15% (w/w).

The suspensions were placed in sealed containers and agitated in a shaker, and pH was measured (Philips DW9418 pH meter) at regular time intervals. After 7 days, 14 days, 28 days and 3 months of hydration time, the suspensions were filtered through 0.45 μm filter paper. The filtration cakes obtained were dried at a temperature of 60 °C for 48 h in a vacuum oven and examined by XRD.

2.2.3. X-ray powder diffraction (XRD)

A Siemens D500 diffractometer and Kristalloflex 810 generator (Cu $K\alpha$ radiation) were used to identify the crystalline products of C_3S hydration. The accelerating voltage was 40 kV and the current was 40 mA. The finely ground samples (<30 μm) were examined between 5° and 40° 2θ at scanning rate of 1° 2θ per minute. The diffractograms were obtained with Diffplus and analysed using Bruker/AXS EVA software and were compared with the current version of the international powder data file (ICDD-JCPDS) for the purpose of phase identification.

2.2.4. Thermal analysis (DTA/TG)

Differential thermal analysis/thermal gravimetry (DTA/TG) techniques are effective tools for analysing the crystalline and amorphous products of cementitious systems. A Stanton Redcroft STA 780 Simultaneous Thermal Analyser was used to conduct DTA/TG analyses of hydrated C_3S pastes with or without heavy metals in this work. The 20 mg of vacuum-drying powdered samples (less than 30 μm) at a temperature of 60 °C for 72 h were packed in the rhodium–platinum crucible of 5.8 mm diameter and 4 mm high. Samples were examined at a heating rate of 10 °C/min under flowing nitrogen (40 cm^3/min) from 30 to 1100 °C. The contents of calcium hydroxide and calcium carbonate were determined from following equations:

$$\text{CH}(\%) = \text{WL}_{\text{CH}}(\%) \times \frac{\text{MW}_{\text{CH}}}{\text{MW}_{\text{H}}} \quad (1)$$

$$\text{CC}(\%) = \text{WL}_{\text{CC}}(\%) \times \frac{\text{MW}_{\text{CC}}}{\text{MW}_{\text{C}}} \quad (2)$$

where CH (%) and CC (%) are the content of $\text{Ca}(\text{OH})_2$ and CaCO_3 , $\text{WL}_{\text{CH}}(\%)$ and $\text{WL}_{\text{CC}}(\%)$ are the weight loss occurred during the decomposition of portlandite and calcium carbonate, MW_{CH} , MW_{H} , MW_{C} and MW_{CC} are the molar weight of portlandite, water, carbon dioxide and calcium carbonate. The mass loss percentages of pure calcium hydroxide and calcite are 24 and 44%, respectively.

2.2.5. Solid-state magic angle spinning/nuclear magnetic resonance

The ^{29}Si chemical shifts in solid-state high resolution magic angle spinning/nuclear magnetic resonance (MAS/NMR) spectroscopy display a regular dependence upon the degree of condensation of silica–oxygen tetrahedra and provide valuable

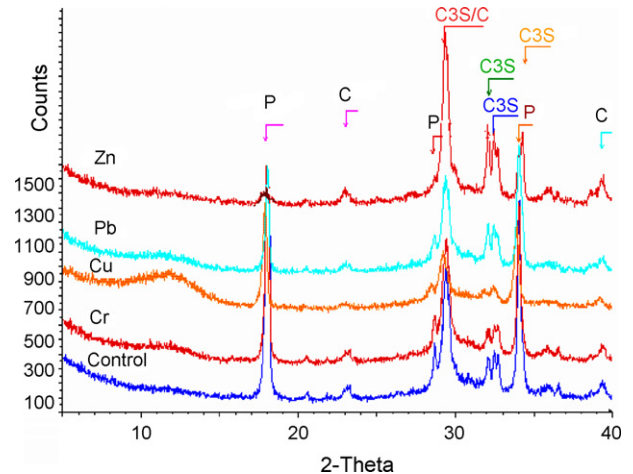


Fig. 2. Diffractograms of 28 days old C_3S hydrated pastes (legend: C: calcite, P: portlandite).

molecular information [19,20]. In this work, ^{29}Si solid-state NMR spectra of hydrated C_3S pastes were recorded on a Varian Infinity Plus-300 spectrometer equipped with a 7.1 T magnet in which the resonance frequency for ^{29}Si is 59.49 MHz. To narrow the resonance peaks, ^{29}Si NMR spectra of hydrated C_3S pastes with or without heavy metals were obtained on a spin rate of 6 kHz. It was operated at relaxation $T_1 \gg 30$ s with a relaxation delay of 10 s. The curing time of all samples for NMR experiments was 1 year after hydration.

3. Results and discussion

3.1. XRD

Fig. 2 presents diffractograms obtained from hydrated C_3S pastes with or without heavy metal at 28 days of age. First of all, it is needed to point out that the diffractograms show the peaks corresponding to calcite, indicating that natural carbonation occurred during the sample preparation and storage, even though the samples were sealed in plastic screw top bottles.

The main differences in diffractograms (Fig. 2) involved the X-ray reflection peaks of portlandite (at 18.1°, 28.5°, 29.5°, and 34° 2θ) and C_3S (at 29.5°, 32°, 32.7°, and 34.4° 2θ). Although the reflection peak intensity is not directly proportional to the content of crystalline phases, some important information can be obtained from comparisons of the relative intensity or changes of the intensity with time. As shown in Fig. 3, the peaks due to portlandite in the control paste were much stronger than those

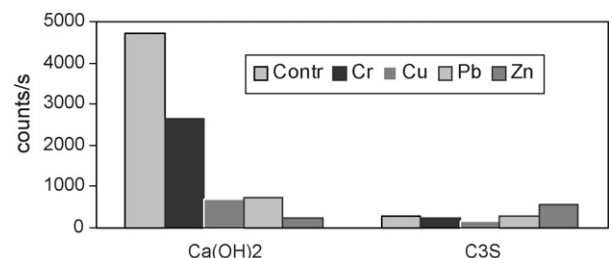


Fig. 3. XRD intensity of main phases in 1-month-old hydrated C_3S pastes.

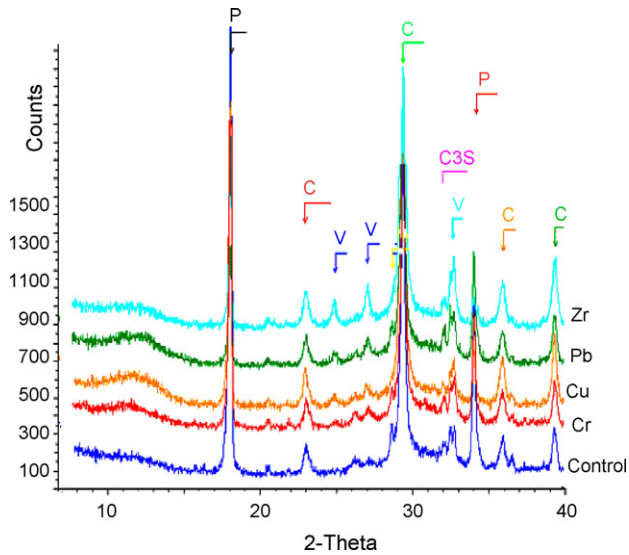


Fig. 4. Diffractograms of 1-year-old hydrated C_3S pastes (legend: C: calcite, P: portlandite, V: vaterite).

in the heavy metal doped pastes, especially in the Zn^{2+} -doped C_3S paste, the X-ray reflection peak at 18.1° due to portlandite was very weak. For the Cu^{2+} -doped, Cr^{3+} -doped C_3S pastes, the X-ray reflection peaks of C_3S were weaker compared with the control paste. However, in the Zn^{2+} -doped C_3S paste, the peaks of C_3S were much stronger than those in the control paste.

Diffractograms of 1-year-old C_3S pastes are shown in Fig. 4. As expected, the relative intensities of C_3S peaks were lower than those of 28 days old C_3S pastes, indicating that hydration had continued with time. Compared with 28 days old hydrated C_3S pastes, the intensities of portlandite peaks in 1-year-old pastes were greater, suggesting that more portlandite precipitated. In addition, more carbonation took place during sample storage, which may have resulted from CO_2 contained in original mix water or from air trapped within the sample bottles. As a consequence, in addition to calcite, which was detected in all the pastes examined, vaterite was observed at 25° , 27.1° and 33° 2θ in Zn^{2+} -doped, Pb^{2+} -doped and Cu^{2+} -doped pastes. The presence of heavy metals influenced the polymorphism of calcium carbonate formed.

In contrast to 28 days old C_3S pastes, the differences of XRD diffractograms of C_3S pastes aged 1 year with or without heavy metals were less pronounced in respect of the reflection peak intensities of C_3S and portlandite. This suggests that the influence of heavy metals on C_3S hydration decreases with time. It is

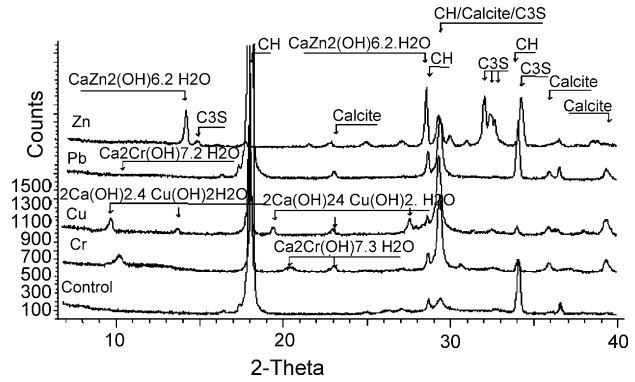


Fig. 5. Diffractograms of products of C_3S suspensions at the age of 3 months (heavy metal/ C_3S : 15%, w/w).

worthy to mention that the increase of heavy metal doping loads in C_3S pastes gave very similar diffractograms described above [21].

Diffractograms obtained from products of C_3S suspension in the presence of heavy metals were much more complex, as shown in Fig. 5. The crystalline products of C_3S suspensions at different hydration time (14 days, 28 days and 3 months) are summarised in Table 1. The X-ray reflection peaks of C_3S in the Cu^{2+} -doped, Cr^{3+} -doped, and Pb^{2+} -doped C_3S systems vanished faster compared with the control sample. In Zn^{2+} -doped C_3S system, the peaks due to C_3S were still very strong even after 3 months (see Fig. 5). According to X-ray reflection peaks of C_3S with time, Cu^{2+} , Pb^{2+} and Cr^{3+} promoted the hydration of C_3S , but Zn^{2+} retarded C_3S early hydration (see Table 1). This opinion is based on the consumption of C_3S in hydration systems and supported by DTA/TG and ^{29}Si NMR results below, differing from the traditional point of view based on hydration heat flow, portlandite contents in pastes or setting time observation in literatures (e.g. [10,17]).

Unlike C_3S pastes containing heavy metals, layered double hydroxides of heavy metal and calcium such as $Ca_2Cr(OH)_7 \cdot 3H_2O$, $Ca_2(OH)_4Cu(OH)_2 \cdot H_2O$ and $CaZn_2(OH)_6 \cdot 2H_2O$ were found to be crystalline phases for C_3S suspensions with heavy metals (Fig. 5). No lead compound was detected, suggesting that Pb was completely absorbed or adsorbed by the products of C_3S hydration due to the relative lower Pb mole concentration in the C_3S suspension. If an initial mole concentration in a C_3S suspension doubled (0.48 M) or increased 4 times (0.96 M, the same mole concentration as other metals), $Pb(OH)_2$ can be detected by XRD (reported elsewhere) [21].

Table 1
The crystalline phase development in C_3S suspensions

Samples	Phases identified by XRD		
	14 days	28 days	3 months
Control	Portlandite, C_3S	Portlandite, C_3S	Portlandite
Cr^{3+} -doped	$Ca_2Cr(OH)_7 \cdot 3H_2O$, portlandite	Portlandite, calcite, $Ca_2Cr(OH)_7 \cdot 3H_2O$	Portlandite, calcite, $Ca_2Cr(OH)_7 \cdot 3H_2O$
Cu^{2+} -doped	Portlandite, $Ca_2(OH)_4Cu(OH)_2 \cdot H_2O$	Portlandite, calcite, $Ca_2(OH)_4Cu(OH)_2 \cdot H_2O$	Portlandite, $Ca_2(OH)_4Cu(OH)_2 \cdot H_2O$ calcite
Pb^{2+} -doped	Portlandite	Portlandite, calcite	Portlandite, calcite
Zn^{2+} -doped	$CaZn_2(OH)_6 \cdot 2H_2O$, C_3S	$CaZn_2(OH)_6 \cdot 2H_2O$, C_3S	$CaZn_2(OH)_6 \cdot 2H_2O$, C_3S , vaterite

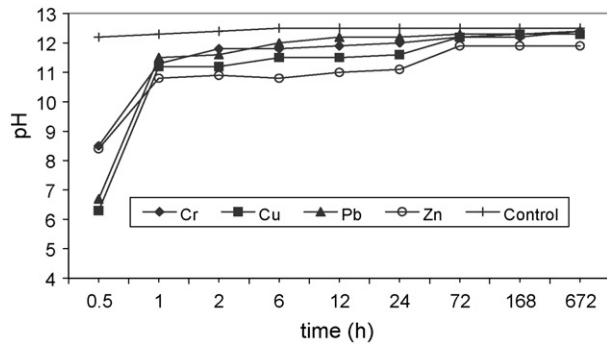


Fig. 6. The pH variation of C_3S suspensions with time.

From XRD patterns of hydration products of C_3S suspensions, it can also be seen that X-ray reflection peaks of portlandite from the control sample was most intensive, in accordance with the hydrated C_3S pastes. Obviously, portlandite did not form in Zn^{2+} -doped C_3S suspension in an early period of hydration time (e.g. 14 days, 28 days and 3 months, see Fig. 5 and Table 1).

3.2. Suspension pH of C_3S

To understand the effects of heavy metals on portlandite precipitation and C_3S hydration, the pH of C_3S suspensions was measured. In the absence of heavy metals, as shown in Fig. 6, C_3S decomposed rapidly and a pH of 12.4 was recorded. This value is close to the pH of the saturated solution of pure portlandite. Additions of heavy metal nitrates decreased pH due to hydrolysis of heavy metal cations. For example, at an initial concentration of 50 g/l (as heavy metal), the initial pH values of C_3S suspensions with Cu^{2+} , Pb^{2+} , Zn^{2+} and Cr^{3+} were 6.3, 6.7, 8.4 and 8.5, respectively. The pH of the C_3S suspensions rose with time due to the hydration of C_3S at different rates, which reflected interactions between C_3S and heavy metals. In Zn^{2+} -doped C_3S suspension, the pH value was below 12 even in 3 months, confirming that Zn^{2+} severely retarded the hydration of C_3S . In low pH media (<12.4), the precipitation of portlandite is inhibited. The suspension pH measurement results can explain that heavy metal doping lowered the amount of portlandite of hydrating C_3S systems. As a result, X-ray reflection peak intensities of portlandite were lower in diffractograms obtained from these materials.

3.3. Thermal analyses

Thermal analysis techniques were used to obtain the further qualitative information and quantitative information (e.g. portlandite contents) of hydrated C_3S pastes with heavy metal. The DTA curves and simultaneous TG curves of C_3S pastes aged 28 days are presented in Figs. 7 and 8. The endothermic peaks in the DTA curves, located at 50–120 °C can be attributed to the evaporation of physically and chemically bound water in C–S–H gel in the pastes [22,23]. The endothermic peaks of portlandite dehydroxylation at 460–510 °C and calcite decomposition at 650–750 °C were observed with an exception of the Zn^{2+} -doped C_3S paste. In the latter, no

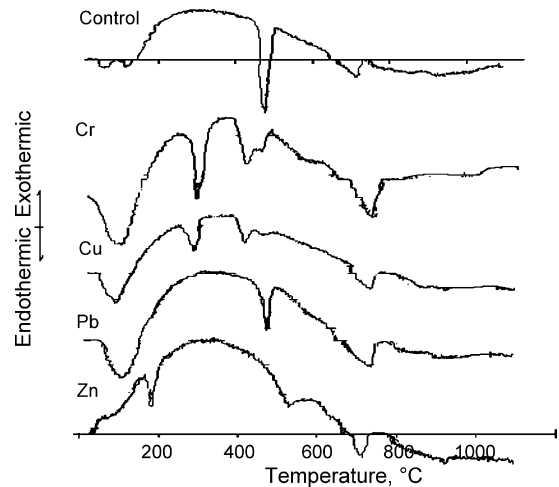


Fig. 7. DTA curves of hydrated C_3S pastes aged 28 days.

endothermic peak of portlandite dehydroxylation at 460–510 °C was observed. The formations of amorphous double hydroxides, such as $Ca_2Cr(OH)_7 \cdot 3H_2O$, $Ca_2(OH)_4Cu(OH)_2 \cdot H_2O$ and $CaZn_2(OH)_6 \cdot 2H_2O$, were responsible for many endothermic reactions occurred during the heating processes. These heavy metal compounds were not detected by XRD in the C_3S pastes but detected as crystals in the C_3S suspensions doped with heavy metal nitrates.

In the control paste, two steps of mass loss in the TG curve corresponding to dehydroxylation of portlandite and decomposition of calcite were very notable. According to the amount of mass loss, the calculated portlandite content and calcite content were 16.7 and 16.8%, respectively (Table 2).

The peaks of DTA/TG curves of the Pb^{2+} -doped C_3S paste were very similar to those of the control paste. The mass loss of portlandite was, however, smaller than that of the control paste. The calculated portlandite content was 7.1% and calculated calcium carbonate content was 27.7%. These results conform to the XRD examinations. Some calcium released from C_3S reactions was consumed due to the formation of calcium carbonate during sample storage and preparation. In other words, the presence of Pb retarded the precipitation of portlandite and accelerated

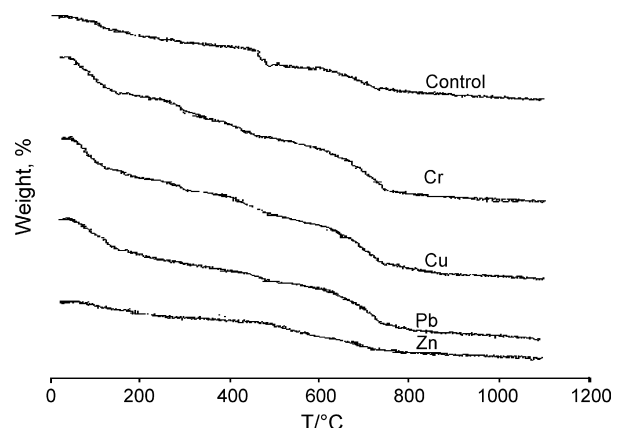


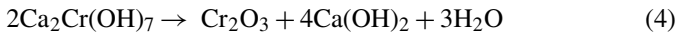
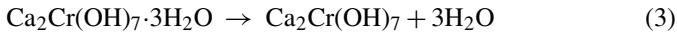
Fig. 8. TG curves of hydrated C_3S pastes aged 28 days.

Table 2
The mass loss and calculated data of hydrated C₃S pastes

Samples	Contr.	Cr ³⁺ -doped	Cu ²⁺ -doped	Pb ²⁺ -doped	Zn ²⁺ -doped
20–250 °C (%)	5.9	12.1	12.3	11.5	4.2
250–600 °C (%)	6.9	12.1	10.7	6.9	4.6
600–900 °C (%)	7.4	12.9	12.9	12.2	5.4
Total mass loss (%)	20.2	37.1	35.9	30.6	14.2
Ca(OH) ₂ (%)	16.7	5.5	5.4	7.1	0.7
CaCO ₃ (%)	16.8	29.3	29.3	27.7	12.3

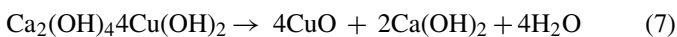
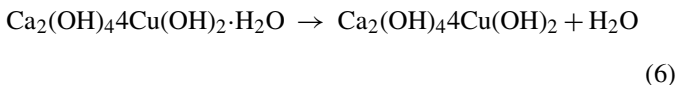
C₃S carbonation due to the lower pH media resulted from the hydrolysis of Pb²⁺ cations.

In the Cr³⁺-doped C₃S paste, there were five major endothermic peaks in the DTA curves, located at 50–120, 280–310, 390–430, 450–500 and 650–780 °C. The decomposition of calcium and chromium double hydroxide is known as following three successive reactions:



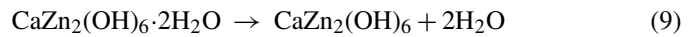
As mentioned earlier, the first endothermic peak can be attributed to the evaporation of physically and chemically bound water in C–S–H gel. The second peak and third peak arose from the dehydration and the decomposition of the double hydroxide of calcium and chromium (Ca₂Cr(OH)₇·3H₂O, Eqs. (3) and (4)). The fourth endothermic peak and corresponding mass loss can be attributed to dehydroxylation of portlandite (Eq. (5)). The fifth endothermic peak at 650–800 °C was due to the decomposition of calcium carbonate. The estimated portlandite content was 5.5%. The calcium carbonate content in the Cr³⁺-doped paste was 29.3%, much higher compared with the control paste (16.8%).

The Cu²⁺-doped C₃S paste also exhibited 5 endothermic peaks. The endothermic peaks in the temperature range of 250–400 and 390–430 °C were due to the decomposition of the double hydroxide (Ca₂(OH)₄Cu(OH)₂·H₂O). The mass loss steps occurred continuously in temperature range of 30–860 °C with different slopes. The endothermic peak and mass loss corresponding to portlandite was very small, the calculated portlandite content and calcium carbonate content were 5.4 and 29.3%, respectively. The decomposition of calcium and copper double hydroxide is shown as following three step reactions:



In the Zn²⁺-doped C₃S paste, there were three endothermic peaks. The second endothermic peak at 170–200 °C could arise from the dehydroxylation of calcium zincate (CaZn₂(OH)₆·2H₂O). The third endothermic peak at

650–800 °C was due to the decomposition of calcium carbonate. The calcium carbonate content, according to the mass loss, was 12.3%. The decomposition of calcium zincate is shown as following equations:



To sum up, the amount of portlandite in C₃S pastes was in the increasing order: control > Pb²⁺ > Cr³⁺ = Cu²⁺ ≫ Zn²⁺, confirming that heavy metals reduced the formation of portlandite during C₃S hydration. This is consistent with the XRD examination, with reference to main peak intensities of portlandite at 18.1° (001), 34.1° (101), 2θ. As all powdered samples investigated were dried at a temperature of 60 °C for 72 h in a vacuum oven, no free water existed and the total mass loss in 100–800 °C should reflect the degree of C₃S reactions (including hydration and carbonation). According to the total mass loss, the reaction degree of C₃S can be arranged in the sequence: Cr³⁺ > Cu²⁺ > Pb²⁺ > control > Zn²⁺. This consequence is also consistent with the XRD examination, with reference to the peaks of C₃S at 32–33° 2θ. It is certain that Cr, Cu and Pb promoted hydration and natural carbonation of C₃S, whereas Zn retarded the early hydration of C₃S.

The retardation effect of Zn on C₃S hydration could arise from the formation of CaZn₂(OH)₆·2H₂O on C₃S surfaces, keeping water from contacting [1,2]. In contrast, double hydroxides (Ca₂Cr(OH)₇·3H₂O and Ca₂(OH)₄Cu(OH)₂·H₂O) formed in Cr³⁺- or Cu²⁺-doped C₃S suspensions may not keep water from contacting C₃S. The reason could be that they may not precipitate on the surface of C₃S or precipitated on the surface of C₃S but did not form membrane or did not cover C₃S grains. The acceleration effect of Cu, Cr and Pb on C₃S hydration could be attributed to the attack of H⁺ resulting from hydrolysis of heavy metal ions, supporting the theory put forward by Taylor [1].

As well known, the solubility of double hydroxide is lower than that of hydroxide in alkaline pH media. The formation of double hydroxides would favour for the reduction of the heavy metal leachability of solidified/stabilised wastes using cement as a binder.

Table 3
²⁹Si NMR data of hydrated C₃S pastes (species proportion, %)

Samples	Control	Cr ³⁺ -doped	Cu ²⁺ -doped	Pb ²⁺ -doped	Zn ²⁺ -doped
Q ⁰ , -72 ppm	16.08	14.97	10.91	15.43	15.2
Q ⁰ , -75 ppm	24.51	24.15	25.40	23.66	20.53
Q ¹ , -80 ppm	32.94	33.53	21.43	34.57	17.86
Q ² , -87 ppm	26.47	27.35	33.33	26.34	34.50
Q ³ , -93 ppm	0	0	8.90	0	11.91
∑Q*	59.41	60.88	63.69	60.91	64.27
α (%)	58.6	60.8	63.4	62.0	65.2
C	1.45	1.44	1.80	1.43	1.82
Ca/Si	1.57	1.56	1.41	1.56	1.36
Psi	3.62	3.66	5.11	3.52	5.86

Note: ∑Q* = Q¹ + Q² + Q³.

3.4. ²⁹Si MAS/NMR spectra

For hydrated C₃S pastes were dominated by C–S–H gel (around 60% by mass), solid-state magic angle spinning/nuclear magnetic resonance (MAS/NMR) was employed to study the structure of calcium silicate gel in the C₃S pastes at the age of 1 year. Based on the ²⁹Si NMR spectra of hydrated C₃S pastes, the differences in the polymerisation of calcium silicate hydrate gel are summarised in Table 3. Note that the hydration degree of C₃S (α), average length (the number of Si) in C–S–H gel (Psi), connectivity ratio (C) and Ca/Si ratio were determined by the following equations [24,25]:

$$\text{Psi} = 2 \left(\frac{1 + I(Q^2)}{I(Q^1)} \right) \quad (12)$$

$$C = \frac{Q^1 + 2Q^2 + 3Q^3 + 4Q^4}{Q^1 + Q^2 + Q^3 + Q^4} \quad (13)$$

$$\frac{\text{Ca}}{\text{Si}} = 2Q^0 + 1.5Q^1 + Q^2 + 0.3Q^3 \quad (14)$$

$$\alpha = \left(\frac{1 - I(Q^0)}{I^0(Q^0)} \right) \times 100\% \quad (15)$$

where $I(Q^0)$, $I(Q^1)$, $I(Q^2)$ are the integral intensity at -75, -80 and -85 ppm, respectively. Q^0 , Q^1 , Q^2 , Q^3 and Q^4 are percentages of respective species. $I^0(Q^0)$ is raw C₃S intensity at -75 ppm.

As shown in Fig. 9, two peaks of C₃S lay at in -72 and -75 ppm, which are characteristic for the mono-silicate group (Q⁰ species) [19]. Hydration of C₃S resulted in transformation of silicate from single tetrahedron (mono-silicate, SiO₄ unit, Q⁰ species) to end groups (Q¹ species) and chain middle groups (Q² species). It is interesting to note that in the control, Cr³⁺-doped and Pb²⁺-doped C₃S pastes, Q¹ > Q², but in Cu²⁺-doped and Zn²⁺-doped pastes, Q² > Q¹, which means a higher condensation of C–S–H gel in the Cu²⁺-doped and Zn²⁺-doped pastes. Correspondingly, the average length (Psi) and values of connectivity (C) of C–S–H gel in the Cu²⁺-doped and Zn²⁺-doped pastes were larger than those of the control paste. In terms of Eq. (12), the numbers of Si in C–S–H gel were 5.86, 5.11, 3.66, 3.62, and 3.52 for the Zn²⁺-doped, Cu²⁺-doped, Cr³⁺-doped, control, and Pb²⁺-doped C₃S pastes, respectively. The calculated Ca/Si

ratios of C–S–H gel in 1-year-old control paste and Zn²⁺-doped, Cu²⁺-doped, Cr³⁺-doped, and Pb²⁺-doped C₃S pastes were 1.57, 1.36, 1.41, 1.56 and 1.56, respectively. In other words, Cu²⁺ and Zn²⁺ doping lowered the Ca/Si ratio of C–S–H gel and promoted the polymerisation of C–S–H gel at age of 1 year compared with the C₃S control paste.

According to ²⁹Si NMR results and Eq. (15), in 1 year of age, all heavy metals investigated slightly promoted the hydration of C₃S in the order: Zn²⁺ > Cu²⁺ > Cr³⁺ > Pb²⁺ > control, although the difference in degrees of C₃S hydration was not very large (2.2–6.6%). As shown in Table 3, the value of α is in good agreement with sum of hydrated species (∑Q* = Q¹ + Q² + Q³), which also describes the proportion of cementitious materials hydrated. The consistency of data from XRD, DTA/TG and NMR indicates that the results of this study are reliable. At present, the mechanism that Zn promoted C₃S hydration in the later period of time (e.g. 1 year) is not known, possibly due to the rupture of calcium zincate membrane on the surfaces of C₃S grains.

In C₃S pastes, calcium silicate hydrate gel (C–S–H) is thermodynamically unstable at ambient temperature, which comprises a large and complex family of phases, with varying compositions. Based on the results of ²⁹Si NMR studies, in the control hydrated C₃S paste, the molecular compositional model of C–S–H gel could be deduced as follows:

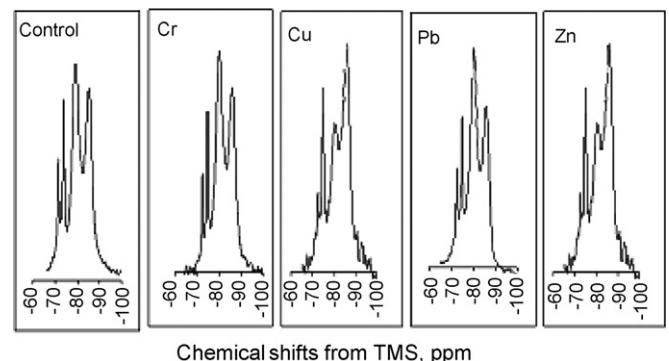
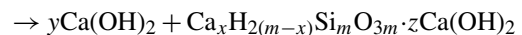
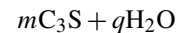
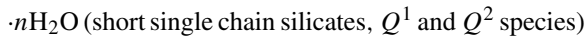
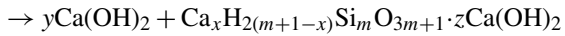
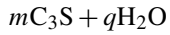


Fig. 9. ²⁹Si NMR spectra of hydrated C₃S pastes.



where $m=3, 4, 5, 6, 7$ (average value: 3.6); $n>0$; $q>0$; $z=0, 1, 2, 3$, etc. $\text{Ca/Si}=(x+z)/m=1.36\text{--}1.57$.

And,



(17)

where $m=2, 3, 4, 5, 6, 7$ (average value: 3.6); $n>0$; $q>0$; $z=0, 1, 2, 3$, etc. $\text{Ca/Si}=(x+z)/m=1.36\text{--}1.57$. If $5-y=x$, it reduces to Glasser's model; If $m=3n-1$, it reduces to the Richardson–Groves' model.

In the presence of heavy metals, hydrolysis of heavy metal cations results in the reduction of pH. But due to C_3S hydration, pH rises, and $\text{M}(\text{OH})_{2(\text{aq})}/\text{M}(\text{OH})_{3(\text{aq})}$ and $\text{M}(\text{OH})_x^{(2 \text{ or } 3-x)}$ ions form. If the amount of heavy metal is large enough and pH is suitable, precipitation of hydroxides and co-precipitation of calcium and heavy metal can occur and form three-dimensional structures. For example, the co-precipitation forms double hydroxides of calcium and copper or chromium, which were identified in this work.

During C_3S hydration, in C–S–H gel, heavy metals may substitute for calcium, or heavy metal hydroxide may substitute for $\text{Ca}(\text{OH})_2$. As a result, the Ca/Si ratio of C–S–H gel in heavy metal doped C_3S pastes decreases. In disordered C–S–H gel, the incorporation of heavy metal is similar to the structure of glass. Heavy metals act as network modifiers or network intermediates.

4. Conclusions

Tricalcium silicate pastes and aqueous suspensions doped with nitrate salts of Zn^{2+} , Pb^{2+} , Cu^{2+} and Cr^{3+} were examined by X-ray powder diffraction (XRD), thermal analysis (DTA/TG) and ^{29}Si solid-state magic angle spinning/nuclear magnetic resonance (MAS/NMR) techniques. The effects of heavy metals on hydrated products of C_3S were recorded and following conclusions can be drawn:

- Heavy metals such as Cu, Cr and Pb promoted hydration of C_3S , whereas Zn exhibited retarding effect at the early period of C_3S hydration. At 1 year, all heavy metals investigated slightly increased the degree of C_3S reactions by 2.2–6.6%.
- XRD and DTA/TG results showed that heavy metals exhibited a retarding effect on precipitation of portlandite and an accelerating effect on the formation of calcium carbonate during C_3S hydration process in the presence of carbon dioxide.
- Double hydroxides of calcium and heavy metals, $\text{Ca}_2\text{Cr}(\text{OH})_7 \cdot 3\text{H}_2\text{O}$, $\text{Ca}_2(\text{OH})_4\text{Cu}(\text{OH})_2 \cdot \text{H}_2\text{O}$ and $\text{CaZn}_2(\text{OH})_6 \cdot 2\text{H}_2\text{O}$, were identified in heavy metal ion doping C_3S suspensions as crystalline phases. In heavy metal doping C_3S pastes the amorphous phases of these compounds were also present according to the thermal analysis results.

- The length of C–S–H gel (the average number of Si) in 1-year-old of hydrated C_3S pastes was in the order: Zn^{2+} (5.86) > Cu^{2+} (5.11) > Cr^{3+} (3.66) > control (3.62) > Pb^{2+} (3.52). Heavy metals, especially Cu and Zn, promoted the polymerisation of C–S–H gel. The Ca/Si ratio of C–S–H gel in 1-year-old of hydrated C_3S pastes was in the range of 1.36–1.57.

Acknowledgements

We warmly thank Drs. C. Macleod and K. Whitehead for their assistance and stimulating discussion. The anonymous referees of the paper are also acknowledged for their constructive criticism and suggestions.

References

- [1] H.F.W. Taylor, Cement Chemistry, Academic Press Limited, London, 1997.
- [2] M. Yousuf, A. Mollah, The interfacial chemistry of solidification/stabilisation of metals in cement and pozzolanic material systems, Waste Manage. 15 (1995) 137–148.
- [3] J.R. Fitch, C.R. Cheeseman, Characterisation of environmentally exposed cement-based stabilised/solidified industrial waste, J. Hazard. Mater. A101 (2003) 239–255.
- [4] H.F.W. Taylor, Nanostructure of C–S–H: current status, Adv. Cem. Basic Mater. 1 (1993) 38–46.
- [5] F.P. Glasser, E.E. Lachowski, D.E. Macphee, Compositional model for calcium silicate hydrate gels, J. Am. Ceram. Soc. 70 (1987) 481–485.
- [6] I.G. Richardson, G.W. Groves, The incorporation of minor trace elements into calcium silicate hydrate gel in hardened cement pastes, Cem. Concr. Res. 23 (1993) 131–138.
- [7] I.G. Richardson, G.W. Groves, The structure of the calcium silicate hydrate phases present in hardened pastes of white Portland cement blast-furnace slag blends, J. Mater. Sci. 32 (18) (1997) 4793–4802.
- [8] I.G. Richardson, The nature of C–S–H in hardened cements, Cem. Concr. Res. 29 (8) (1999) 1131–1147.
- [9] I.G. Richardson, Tobermorite/jennite and tobermorite/calcium hydroxide-based models for the structure of C–S–H: applicability to hardened pastes of tricalcium silicate, h-dicalcium silicate, Portland cement, and blends of Portland cement with blast-furnace slag, metakaolin, or silica fume, Cem. Concr. Res. 34 (2004) 1733–1777.
- [10] J.R. Conner, Chemical Fixation and Solidification of Hazardous Waste, Van Nostrand Reinhold, New York, 1990.
- [11] F.P. Glasser, Fundamental aspects of cement solidification and stabilisation, J. Hazard. Mater. 52 (1997) 151–170.
- [12] M. Murat, F. Sorrentino, Effect of large addition of Cd, Pb, Cr, Zn to cement raw meal on the composition and the properties of the clinker and the cement, Cem. Concr. Res. 26 (1996) 377–385.
- [13] D. Stephan, H. Maleki, D. Knoefel, Influence of Cr, Ni, and Zn on the properties of pure clinker phases, Part 1. C_3S , Cem. Concr. Res. 29 (1999) 545–552.
- [14] D. Bonen, S.L. Sarkhar, The effects of simulated environmental attack on immobilisation of heavy metals doped in cement-based materials, J. Hazard. Mater. 40 (1995) 321–335.
- [15] D. Cocke, J.D. Ortego, A model for lead retardation of cement setting, Cem. Concr. Res. 19 (1989) 156–159.
- [16] D.A. Thomas, D.A. Jameson, D.D. Double, The effect of lead nitrite on the early hydration of Portland cement, Cem. Concr. Res. 11 (1981) 143–153.
- [17] C.D. Hills, S.J.T. Pollard, The influence of interference effects on the mechanical, micro-structural and fixation characteristics of cement-solidified waste forms, J. Hazard. Mater. 52 (1997) 171–191.
- [18] X.C. Qiao, C.S. Poon, C.R. Cheeseman, Investigation into the stabilization/solidification performance of Portland cement through cement clinker phases, J. Hazard. Mater. 139 (2007) 238–243.

- [19] E. Lippmaa, M. Magi, M. Tarmak, A high resolution ^{29}Si NMR study of the hydration of tricalcium silicate, *Cem. Concr. Res.* 12 (1982) 597–602.
- [20] X.D. Cong, R.J. Kirkpatrick, ^{29}Si MAS NMR study of the structure of calcium silicate hydrate, *Adv. Cem. Based Mater.* 3 (3–4) (1996) 144–156.
- [21] Q.Y. Chen, Examination of hydrated and carbonated mixtures of cement and metals, Ph.D. Thesis, The University of Greenwich, London, 2004.
- [22] J. Dweck, P.M. Buchler, Hydration of Portland cement blended with calcium carbonate, *Thermochim. Acta* 346 (2000) 105–113.
- [23] J. Dweck, P.E.F. da Silva, R.S. Aderne, Evaluating cement hydration by non-conventional DTA—an application to waste solidification, *J. Therm. Anal. Calorim.* 71 (3) (2003) 821–827.
- [24] C.K. Lin, J.N. Chen, C.C. Li, NMR, XRD and EDS study of solidification/stabilisation of chromium with Portland cement and C3S, *J. Hazard. Mater.* 56 (1997) 21–34.
- [25] G.K. Sun, A.R. Brough, J.F. Young, ^{29}Si NMR study of the hydration of Ca_3SiO_5 and Ca_2SiO_4 in the presence of silica fume, *J. Am. Ceram. Soc.* 82 (11) (1999) 3225–3230.